Water-jet Assisted Nanosecond Laser Microcutting of Northeast China Ash Wood: Experimental Study

Chunmei Yang,[a,b] Ting Jiang,[a,b,]* Yueqiang Yu,[a] Yan Bai,[a] Mingliang Song,[a,b] Qian Miao,[a,b] Yan Ma,[a,b,]* and Jiuqing Liu [a,]*

Laser machining is an advanced technology that provides efficiency and precision for the processing of wood. In this paper, the ablation mechanism of wood processed *via* a water-jet assisted nanosecond laser was analyzed. The influences of cutting speed and laser power on the cutting width of northeast China ash wood (NCAW) (*Fraxinus mandshurica* Rupr.) with and without the water-jet assisted system were evaluated. The surface morphology of the kerf of processed NCAW was observed *via* scanning electron microscopy (SEM). Furthermore, a factorial design experiment was carried out to analyze the effects of process parameters on the cutting width. Additionally, the experimental results were processed by multilinear regression analysis. The results showed that with the water-jet assisted system, the minimum value of the cutting width was 0.18 mm when the cutting speed was 50 mm/s and the laser power was 6 W, and good surface quality was obtained. The experimental results were processed by an analysis of variance and multilinear regression analysis. The predicted model, effectively validated by the experiments, had good prediction accuracy, which provided a theoretical basis for predicting the cutting width of NCAW processed by a water-jet assisted laser.

Keywords: Nanosecond laser; Water-jet assisted system; Northeast China ash wood; Factorial design experiment; Micromorphology

Contact information: a: Northeast Forestry University, College of Mechanical and Electrical Engineering, Harbin, 150040, China; b: Forestry and Woodworking Machinery Engineering Technology Center, Northeast Forestry University, Harbin 150040, China;
** Corresponding authors: jiangting1112@163.com; ycmnefu@126.com; nefujdljq@163.com*

INTRODUCTION

Wood is a natural and environmentally friendly material that is widely used in the construction, packing, furniture, and flooring industries (Fleming *et al*. 2003; Seo *et al*. 2011; Fukuta *et al*. 2016a). Because of its widespread use, improving the utilization ratio of wood resources has become the focus of researchers. The tools used in traditional processes have a certain geometric shape, which leads to the waste of wood resources in the process of wood processing. The saw dust left over after processing also pollutes the environment. Laser processing technology has advantages over traditional processes, including high efficiency, no noise, and narrow cutting width, which makes up for the deficiency of traditional processes. Therefore, it is widely used in fields such as cutting, engraving, and surface treatment of wood and wood composites (Barcikowski *et al*. 2006; Leone *et al.* 2009; Eltawahni *et al.* 2011; Vidholdová *et al*. 2017).

Recently, researchers have gradually focused on fine processing of wood. Nukman *et al*. (2008) investigated CO_2 laser cutting of Malaysian hardwood. They outlined the relationship between processing parameters and types of wood with different properties in terms of optimum cutting conditions. Additionally, they showed that an acceptable surface was obtained when nitrogen was used to assist the cutting process. Fukuta *et al*. (2016b and 2016c) used solid-state lasers, short-wavelength lasers, to process wood to obtain precise machining because short wavelengths allowed for a smaller theoretical focal diameter. In addition, short-pulse lasers allowed heat effects to the surrounding area to be controlled while increasing the peak power. Hernández-Castañeda *et al*. (2011) concluded that cutting wet pine wood with a fiber laser produced narrower cutting kerf and a smoother surface in comparison with dry samples. However, after the wood was cut with a laser, assisting gas could not fully keep residues away from the wood surface, which affected the surface quality. Therefore, in the author's previous research, a water jet assisted nanosecond laser was used to process Korean pine to improve its surface quality. This was mainly because the cooling and washing effects of water-jet had reduced heat-affected zone and washed away the residues on the surface of the Korean pine, which avoided the process defect of traditional laser (Yang *et al*. 2018). However, different species of wood have different physical and chemical properties that directly affect the surface quality of the wood. The authors found no research that has investigated the machining of hardwood processed by a water-jet assisted nanosecond laser. Northeast China ash wood (NCAW) is a type of precious hardwood tree in northeast China with a high density. It is widely applied in the furniture industry because of its beautiful texture and good resistance to decay.

Therefore, this paper analyzes the ablation mechanism of wood processed by a water-jet assisted nanosecond laser. A single factor experiment and a factorial design experiment were performed to evaluate the influences of laser power and cutting speed on the cutting width of NCAW with and without the water-jet assisted system. Furthermore, the surface quality of NCAW after cutting was assessed, and the prediction model of multilinear regression was established. This research provided a foundation for the prediction of the cutting width of NCAW processed by a water-jet assisted nanosecond laser.

PROCESS MECHANISM

The ablation mechanism diagram of wood processed by a water-jet assisted nanosecond laser is shown in Fig. 1. In the machining process, the high energy density of the laser beam rapidly focuses on the processing region of the wood. The decomposition of lignin starts at approximately 280 °C (Nassar and MacKay 1984). Therefore, the internal moisture within the wood cell evaporated quickly, which resulted in empty tracheids. Due to a rapid change of temperature, a great thermal stress gradient occurred around the processing region. At the same time, local expansion and contraction took place in the substrate of the wood. Hence, microcracks caused by residual stress appeared. Furthermore, due to the lower ignition temperature of wood, part of the laser energy density in the processing zone was always lower than the laser energy density for the vaporization of wood, causing the burning of wood. Thus, carbonization and ablation of the heat-affected zone (HAZ) are observed, along with residuals, such as carbon granules, charring, and ash content, which has a negative impact on the surface quality of wood (Panzner *et al*. 1998; Yue *et al*. 2013; Kubovský and Kačík 2014; Yu *et al*. 2015). However, water jets not only can reduce the heat-affected zone and microcracks, they also effectively take away residuals, thus improving the surface quality of wood processed by water-jet assisted nanosecond lasers.

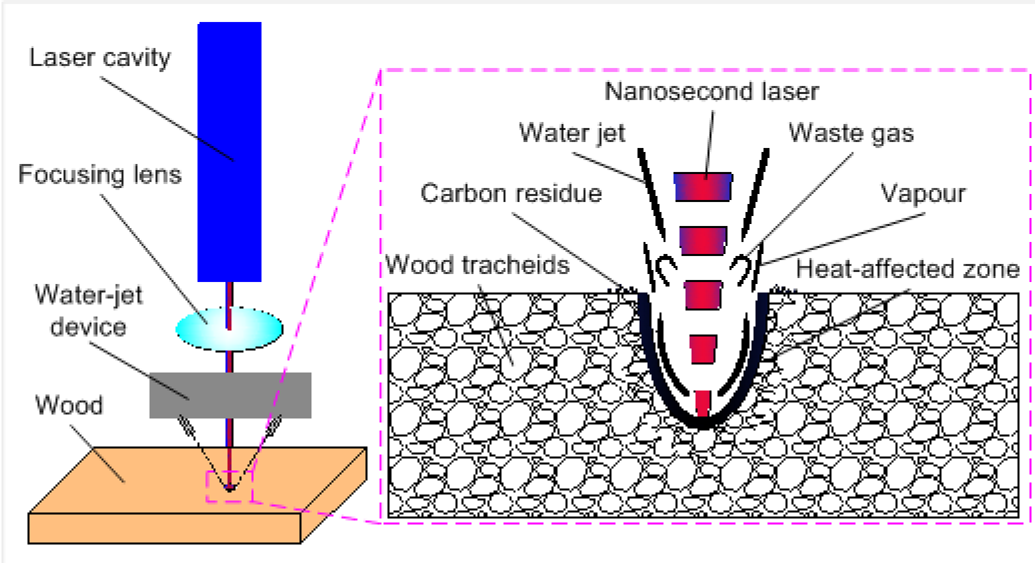

Fig. 1. The ablation mechanism diagram of wood processed by water-jet assisted nanosecond laser

EXPERIMENTAL

Materials and Experimental Setup

The NCAW, belonging to a typical hardwood, was used as the experimental material (Haicheng Machining Factory, Harbin, China). The NCAW has an air-dry density of 0.70 g/cm^3 and a moisture content of 12.32%. A NCAW with the same size was obtained after processing, and the size was 100 mm × 60 mm × 2 mm (length × width × thickness).

The experimental setup is shown in Fig. 2.

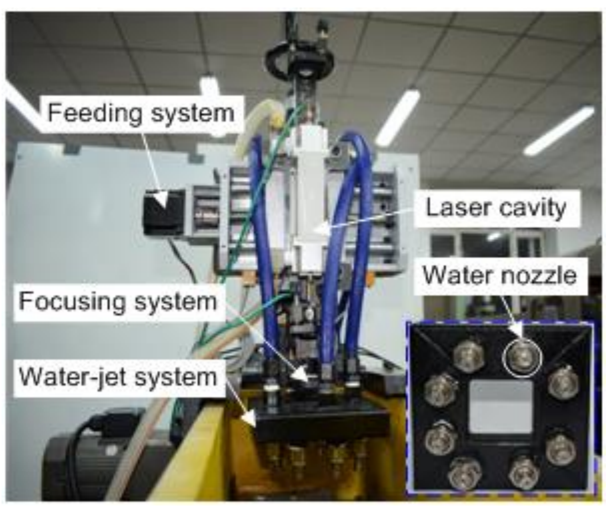

Fig. 2. Experimental setup

The laser system contained a Nd:YAG (Neodymium Doped Yttrium Aluminum Garnet) laser (Dongjun Laser Co., Ltd., Chengdu, China), a JDW3-250 laser power supply

(Dongjun Laser Co., Ltd., Chengdu, China), and a PH-LW06-BLP laser cooling system (Dongluyang Co., Ltd., Shenzhen, China). The water-jet assisted system consisted mainly of annular nozzles. The feeding system moved through the X-axis, Y-axis, and Z-axis. The focusing system consisted of a combination of optical lenses.

The wavelength of the laser was 1064 nm, the pulse width was 20 ns, and the pulse repetition rate was in the range of 1 kHz to 10 kHz. The focal length of the focusing lens was 100 mm. The focused beam spot size was 0.05 mm. The angle of water jet could be adjusted to control the range of the water ring. The adjustable nozzle flow pressure was set as 0.13 MPa. The water flow of the water-jet system was 8 m^3/ h, and the water-jet speed was 5.75 m/s.

Methods

The process direction was along the NCAW fiber. The specimen and process method are shown in Fig. 3. The focused beam spot was located on the top of the surface of the NCAW. The cutting width was the average of the widths on the top and bottom surfaces along the thickness direction, which were measured using an optical microscope (JNOEC XS213, Tianlong Instrument Factory, Nanjing, China). The tangential section of the processed NCAW with and without water-jet assist was observed using a FEI Quanta200 scanning electron microscope (FEI Instruments, Hillsboro, OR, USA).

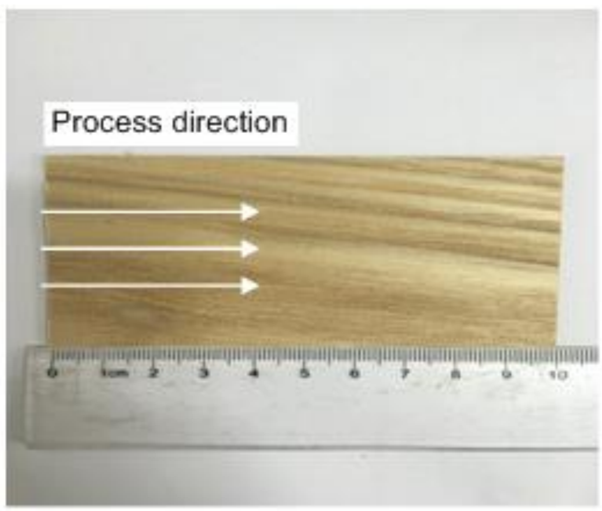

Fig. 3. Specimen and process method

Design of two-factor experiment

A two-factor experiment was performed. The NCAW was processed with and without water-jet assisted nanosecond laser. The pulse repetition rate was chosen as 1 kHz. The process parameters are shown in Table 1. The change tendencies of process parameters on the cutting width of NCAW were studied.

Table 1. Processing Parameters of Nanosecond Laser Processing

Sample Number	1	2	3	4	5	6	7	8	9	10
Avg. Laser Power (W)	6	8	10	12	14	16	18	20	22	24
Cutting Speed (mm/s)	5	10	15	20	25	30	35	40	45	50

Factorial design experiment

Then, a factorial design experiment was performed by software (SPSS Statistics, IBM, 23.0, New York, USA) and the influence rules of the multiple process parameters and their effects on the surface quality of NCAW were studied. Through a factorial design experiment, the influence rules of the laser power (high, medium, and low levels), cutting speed (high, medium, and low levels), and water-jet speed (with and without) on the cutting width of NCAW were studied. The influence of the water-jet system on the surface quality of NCAW was also studied. A 2 × 3 × 3 factorial design was performed with 18 groups and with average value of three cutting tests in each group. The factors and levels of factorial design are shown in Table 2.

Table 2. Factors and Levels of Factorial Design

Factors \ Levels	1	2	3
A (Water-jet Speed, m/s)	0 (A_0)	5.75 (A_1)	-
B (Laser Power, W)	8 (B_1)	14 (B_2)	20 (B_3)
C (Cutting Speed, mm/s)	10 (C_1)	25 (C_2)	40 (C_3)

RESULTS AND DISCUSSION

Effect of Laser Powers and Cutting Speeds on Cutting Width of NCAW

The process parameters of the two factors experiment with the water-jet assisted nanosecond laser are shown in Table 1. The NCAW was processed by a nanosecond laser with or without the water-jet assisted system. The cutting width data under various average laser powers and cutting speeds was processed. The change tendencies are shown in Fig. 4, which illustrates that the change tendencies of the cutting width with different laser powers and cutting speeds were consistent with and without the water-jet assisted system.

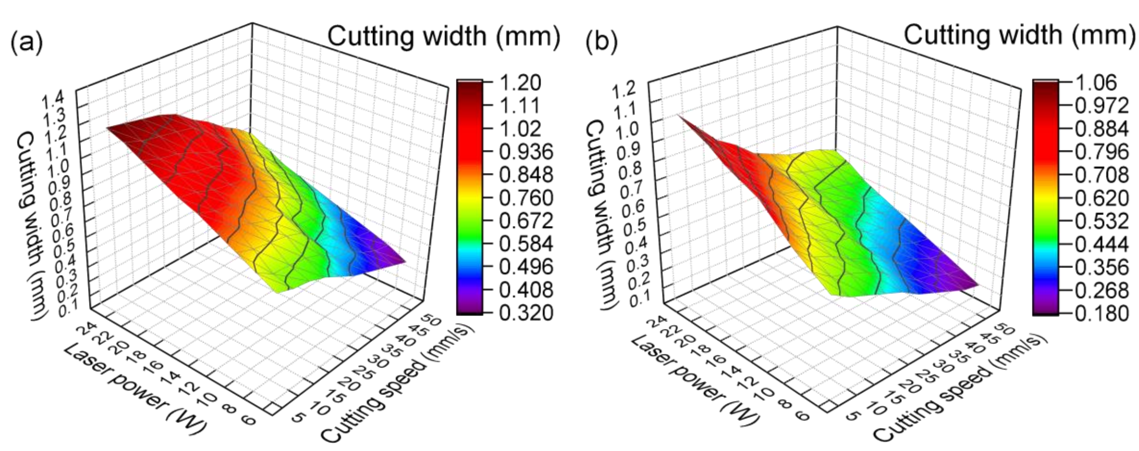

Fig. 4. The cutting width difference under various laser powers and cutting speeds for NCAW, (a) without or (b) with the water-jet assisted system

When the cutting speeds were constant, the cutting width increased with an increase in laser power. A lower laser power caused less heat on the surface of the NCAW; with less sublimation and burning, less NCAW was removed. Hence, the cutting width was small. An increased laser power generated more heat on the NCAW surface, which caused its temperature to rise rapidly. The NCAW sublimated and formed the cutting width; thus, the large consumption of NCAW caused an increased cutting width. When the laser power was constant, the cutting width decreased with an increase in the cutting speed. When the cutting speed was low, a longer interaction between the laser beam and NCAW caused a large heat accumulation effect on NCAW, which was followed by an increase in the heat-affected zone and cutting width. With an increase in cutting speed, less heat from the laser beam accumulated on the NCAW in the unit time, which caused the cutting width to decrease accordingly. Figure 4 shows that when the cutting speed was 50 mm/s and the laser power was 6 W, the smallest cutting width of NCAW was 0.32 mm without the involvement of a water-jet assisted system. However, the smallest cutting width of NCAW was 0.18 mm when the water-jet assisted system was involved, which resulted in the minimum cutting width and highest size precision. Under the water-jet assisted system, the high temperature produced by the laser beam was cooled, and the range of the heat-affected zone was reduced. At the same time, the water-jet continuously flowed, which also cleared the residues on the cutting surface. Therefore, its minimum cutting width was smaller than when the water-jet assisted system was not used.

Analysis of Variance for Cutting Width of NCAW

For the process involving the use of a water-jet assisted nanosecond laser, the factorial design experimental results are shown in Table 3.

Table 3. Factorial Design Experimental Results for Cutting Width of NCAW

$A \times B$		C_1			C_2			C_3		
B_1	A_0	0.68	0.65	0.74	0.63	0.66	0.57	0.45	0.49	0.41
	A_1	0.51	0.59	0.55	0.48	0.39	0.42	0.24	0.32	0.28
B_2	A_0	0.88	0.86	0.96	0.79	0.87	0.80	0.58	0.68	0.63
	A_1	0.77	0.68	0.71	0.57	0.60	0.51	0.38	0.46	0.36
B_3	A_0	1.04	1.12	1.02	0.93	1.01	0.91	0.77	0.75	0.85
	A_1	0.83	0.92	0.86	0.64	0.72	0.68	0.54	0.47	0.49

The analysis of variance for the experimental results was conducted by software (SPSS Statistics, IBM, 23.0, New York, USA). The significant factors were determined (Table 4). It can be seen that $A*C$ (F = 3.000, Sig. = 0.062 > α = 0.05), $B*C$ (F = 0.880, Sig. = 0.486 > α = 0.05), and $A*B*C$ (F = 0.267, Sig. = 0.897 > α = 0.05) had no significant effect on the cutting width. For the convenience of calculation, these interactions between factors were not considered in the multilinear regression analysis. However, the other factors (*A*, *B*, *C*) and the interaction between (*A**B*), whose main effects were statistically significant, were considered to be the main effect factors for the cutting width of NCAW.

Table 4. Analysis of Variance for Cutting Width Under Process Parameters

Source	Sum of Squares	Degrees of Freedom	Mean Square	F	Sig.
Corrected Model	2.257	17	0.133	61.755	0.000
Intercept	23.602	1	23.602	10977.519	0.000
A	0.614	1	0.614	285.767	0.000
B	0.840	2	0.420	195.403	0.000
C	0.763	2	0.382	177.543	0.000
A*B	0.016	2	0.008	3.791	0.032
A*C	0.013	2	0.006	3.000	0.062
B*C	0.008	4	0.002	0.880	0.486
A*B*C	0.002	4	0.001	0.267	0.897
Error	0.077	36	0.002		
Total	25.936	54			
Corrected Total	2.335	53			

Multilinear Regression Analysis for Cutting Width of NCAW

To further clarify the relationship between the process parameters and the cutting width of NCAW, a multilinear regression method was used to establish the selection of the model of factors and the cutting width. The multilinear regression model reflected the interaction effects of various factors on the cutting width. Some significant factors stood out, and other non-significant factors could be deleted.

The regression model established through the sample data could not be immediately used for analysis and prediction of the actual problem; thus, a variety of statistical tests needed to be conducted, such as the goodness of fit test (Table 5), F-test (Table 6), and T-test (Table 7).

Table 5. Goodness of Fit Test

R	R^2	Adjusted R^2	Standard Error of Estimate
0.993	0.985	0.981	0.029

Table 6. F-test

Model	Sum of Squares	Degrees of Freedom	Mean Square	F-value	Sig.
Regression	0.741	4	0.185	219.156	0.000
Residual	0.011	13	0.001		
Total	0.752	17			

Table 7. T-test

Model	Non-standardized Coefficients		Standardized Coefficient	T-value	Sig.
	B	Standard Error			
Constant	0.605	0.033		18.607	0.000
A	-0.020	0.007	-0.284	-2.797	0.015
B	0.029	0.002	0.692	14.600	0.000
C	-0.010	0.001	-0.579	-17.272	0.000
*A*B*	-0.001	0.000	-0.265	-2.482	0.028

In Tables 5 through 7, regression models were processed according to a goodness of fit test, F-test, and T-test, respectively. Compared with the non-standardized coefficients of each factor, the model of the cutting width of NCAW under process parameters can be expressed as:

$$T = 0.605 - 0.02A + 0.029B - 0.01C - 0.001A*B \quad (1)$$

In Eq. 1, the regression coefficient of the water-jet speed had a negative value, which indicated that water-jet speed had the opposite effect on the cutting width of NCAW. With the increase of the water-jet speed and cutting speed, the cutting width of NCAW decreased.

A synergistic effect was decreased, and an antagonistic effect was increased in the system; the regression coefficient of the water-jet speed had a positive value, which represented that the water-jet speed had a better effect on the cutting width of NCAW. With the increase of the laser power, the cutting width of NCAW increased. The binary interaction effect of *A**B* on the cutting width of NCAW was significant; however, the ternary interaction effect was not significant. The regression coefficient of *A**B* had a negative value, which indicated that *A**B* had an opposite effect on the cutting width of NCAW, which was shown as an antagonistic effect in the system.

Validity of Predicted Model

The NCAW was processed by a water-jet assisted nanosecond laser, and the obtained measured value of the cutting width was compared with the predicted value of the cutting width. Thus, the prediction accuracy of the established multilinear regression model of the cutting width was tested. Five test samples in the process parameters of the water-jet assisted laser were randomly selected. Then, these process parameters were brought to the prediction model, as shown in Eq. 1, where the model prediction value of the cutting width of the corresponding process parameters could be obtained

The comparison of the measured value and the model predictive value of the cutting width is shown in Table 8. The error range of the prediction value of the cutting width was within ± 7%, and the average prediction error was 4.152%. This showed that the prediction model of the multilinear regression of the cutting width was precise. Therefore, the influence of the process parameters by the water-jet assisted nanosecond laser on the cutting width was well described.

Table 8. Comparison of the Measured and Predicted Values of Cutting Width

Sample Number	Water-jet Speed (m/s)	Laser Power (W)	Cutting Speed (mm/s)	Cutting Width (mm)		Relative Error (%)
				Measured value	Predicted value	
1	0	6	10	0.66	0.68	3.03
2	5.75	10	20	0.50	0.52	4.00
3	0	16	30	0.82	0.77	6.10
4	5.75	18	5	0.92	0.86	6.52
5	0	22	35	0.90	0.89	1.11

Micromorphology of the Kerf Surface of NCAW

The surface quality of machining parts is an important factor that affects the performance of the parts and is an important index for evaluation of the process technology. Thus, the surface quality of the parts was studied. Tangential section micromorphology of NCAW when the cutting width was minimum, without and with the water-jet assisted system, was observed under SEM (Fig. 5). As shown in Fig. 5a, there were some residues and cracks left on the kerf surface of NCAW after the laser process, and the cutting surface was rough. Thus, the surface quality was bad. In Fig. 5b, there were no residues and cracks left on the kerf surface of NCAW after the laser process with the water-jet assisted system, and the cutting surface was smooth; thus, the surface quality was better. This was because of the cooling of the water-reduced cracks caused by the accumulation of heat. At the same time, the water flow washed away the residues that remained on the kerf surface of NCAW. Therefore, the surface quality of the cutting processed by the laser with the water-jet assisted system was better than the surface quality of cutting processed without the water-jet assisted system.

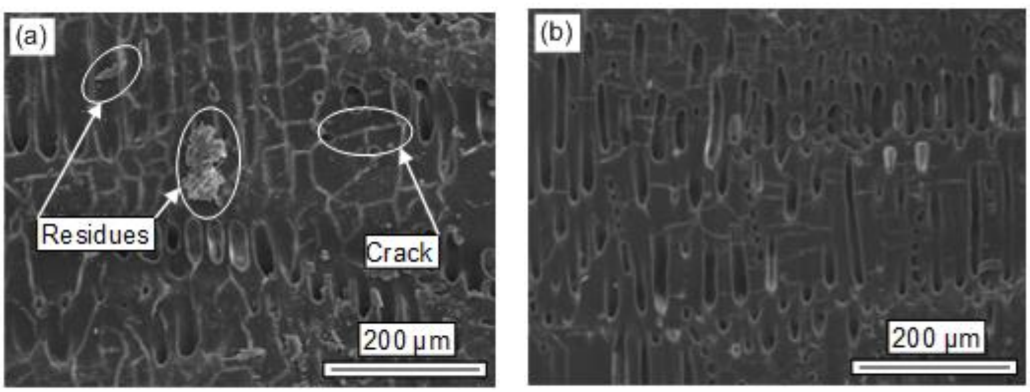

Fig. 5. Tangential section micromorphology of NCAW when cutting width was minimum under 100 times; (a) without and (b) with the water guided system

CONCLUSIONS

1. Based on the analysis of the ablation mechanism of wood, a water-jet assisted nanosecond laser was used to process NCAW. The experimental results showed the influence of the cutting speed and the laser power on the cutting width. When the cutting speed was constant, the cutting width increased with the increase of laser power. When the laser power was constant, the cutting width decreased with the increase of cutting speed. When the cutting speed was 50 mm/s and the laser power was 6 W, the cutting width of 0.18 mm under the water-jet assisted system was smaller than the cutting width produced without the water-jet assisted system.
2. Through an analysis of variance of a factorial design of the experiment, the effects of water-jet speed, laser power, cutting speed, and the interaction of water-jet speed and laser power on cutting width were significant. A multivariate linear regression method was used to establish the model of selected factors and the cutting width of NCAW. The predicted model of the process parameters and cutting width by water-jet assisted nanosecond laser was obtained. After validation, the prediction model had good predictive precision.

3. The kerf surfaces of NCAW were observed *via* SEM. Without the water-jet assisted system, there were some residues and cracks left on the kerf surface of NCAW, which resulted in a rough surface. Thus, the surface quality was bad. With the water-jet assisted system, no residues and cracks were left on the kerf surface of NCAW, and the kerf surface was smooth. Hence, the surface quality of the NCAW processed by laser with the water-jet assisted system was better than the surface quality of the NCAW processed without the water-jet assisted system.

ACKNOWLEDGMENTS

The authors are grateful for the Fundamental Research Funds for the Central Universities (No. 2572018AB25), the Special Fund for the Continued Development of High-level Talent (No. 2572018CG06) and the Fundamental Research Funds for the Central Universities (No. 2572016EBC3).

REFERENCES CITED

Barcikowski, S., Koch, G., and Odermatt, J. (2006). "Characterization and modification of the heat affected zone during laser material processing of wood and wood composites," *Holz. Roh. Werkst.* 64(2), 94-103. DOI: 10.1007/s00107-005-0028-1

Eltawahni, H. A., Olabi, A. G., and Benyounis, K. Y. (2011). "Investigating the CO_2 laser cutting parameters of MDF wood composite material," *Opt. Laser Technol.* 43(3), 648-659. DOI: 10.1016/j.optlastec.2010.09.006

Fleming, M. R., Hoover, K., Janowiak, J. J., Fang, Y., Wang, X., Liu, W., Wang, Y., Hang, X., Agrawal, D., Mastro, V., *et al.* (2003). "Microwave irradiation of wood packing material to destroy the Asian longhorned beetle," *Forest Prod. J.* 53(1), 46-52.

Fukuta, S., Ogawa, K., Nomura, M., Yamasaki, M., and Sasaki, Y. (2016a). "Sound insulation of walls using wood insulation mat and plywood jointed with a combination of adhesive tape and wood dowels," *Eur. J. Wood Wood Prod.* 75(4), 595-602. DOI: 10.1007/s00107-016-1085-3

Fukuta, S., Nomural, M., Ikeda, T., Yoshizawa, M., Yamasaki, M., and Sasaki, Y. (2016b) "Wavelength dependence of machining performance in UV-, VIS- and NIR-laser cutting of wood," *J. Wood Sci.* 62(4), 316-323.DOI 10.1007/s10086-016-1553-8

Fukuta, S., Nomural, M., Ikeda, T., Yoshizawa, M., Yamasaki, M., and Sasaki, Y. (2016c) "UV laser machining of wood," *Eur. J. of Wood and Wood Prod.* 74(2), 261-267. DOI 10.1007/s00107-016-1010-9

Hernández-Castañeda, J. C., Sezer, H. K., and Li, L. (2011). "The effect of moisture content in fibre laser cutting of pine wood," *Opt. Laser Eng.* 49(9–10), 1139-1152. DOI: 10.1016/j.optlaseng.2011.05.008

Kubovský, I., and Kačík, F. (2014). "Colour and chemical changes of the lime wood surface due to CO_2 laser thermal modification," *Appl. Surf. Sci.* 321, 261-267. DOI: 10.1016/j.apsusc.2014.09.124

Leone, C., Lopresto, V., and Iorio, I. D. (2009). "Wood engraving by Q-switched diode-pumped frequency-doubled Nd:YAG green laser," *Opt. Laser Eng.* 47(1), 161-168. DOI: 10.1016/j.optlaseng.2008.06.019

Nassar, M. M., and MacKay, G. D. M. (1984). "Mechanism of thermal decomposition of lignin," *Wood Fiber Sci.* 16(3), 441–453.

Nukman, Y., Ismail, S. R., Azuddin, M., and Aznijar, A. Y. (2008). "Selected Malaysian wood CO_2-laser cutting parameters and cut quality," *Am. J. Appl. Sci.* 5(8), 990-996. DOI: 10.3844/ajassp.2008.990.996

Panzner, M., Wiedemann, G., Henneberg, K., Fischer, R., Wittke, T., and Dietsch, R. (1998). "Experimental investigation of laser ablation process on wood surfaces," *Appl. Surf. Sci*. 127–129, 787-792. DOI: 10.1016/S0169-4332(97)00743-5

Seo, J., Jeon, J., Lee, J. H., and Kim, S. (2011). "Thermal performance analysis according to wood flooring structure for energy conservation in radiant floor heating systems," *Energ. Buildings* 43(8), 2039-2042. DOI: 10.1016/j.enbuild.2011.04.019

Vidholdová, Z., Reinprecht, L., and Igaz, R. (2017). "The impact of laser surface modification of beech wood on its color and occurrence of molds," *BioResources* 12(2), 4177-4186. DOI: 10.15376/biores.12.2.4177-4186

Yang, C. M., Jiang, T., Yu, Y. Q., Dun, G. Q., Ma, Y., and Liu, J. Q. (2018). "Study on surface quality of wood processed by water-jet assisted nanosecond laser," *BioResources* 13(2), 3125-3134. DOI: 10.15376/biores.13.2.3125-3134

Yu, M., Song, S., Jiang, S. H., Ma, Y., and Ren, H. E. (2015). "Theory research of wood surface cells explosion heated by nanosecond laser," *Forestry Machinery and Woodworking Equipment* 43(2), 30-32. DOI: 10.13279/j.cnki.fmwe.2015.0026

Yue, W., Ando, K., and Hattori, N. (2013). "Changes in the anatomy of surface and liquid uptake of wood after laser incising," *Wood Sci. Technol.* 47(3), 447-455. DOI: 10.1007/s00226-012-0497-4

Article submitted: July 28, 2018; Peer review completed: September 17, 2018; Revised version received and accepted: November 1, 2018; Published: November 13, 2018.
DOI: 10.15376/biores.14.1.128-138